the plant journal

SEB Society for Experimental Biology

The Plant Journal (2017) **90,** 1040–1051 doi: 10.1111/tpj.13516

OsNLA1, a RING-type ubiquitin ligase, maintains phosphate homeostasis in *Oryza sativa* via degradation of phosphate transporters

Wenhao Yue[1,†], Yinghui Ying[1,†], Chuang Wang[1,‡], Yang Zhao[1], Changhe Dong[1], James Whelan[2] and Huixia Shou[1,*]

[1]*State Key Laboratory of Plant Physiology and Biochemistry, College of Life Sciences, Zhejiang University, 866 Yuhangtang Road, Hangzhou 310058, P. R. China, and*

[2]*ARC Centre of Excellence in Plant Energy Biology, Department of Animal, Plant and Soil Science, School of Life Science, La Trobe University, Victoria 3086, Australia*

Received 14 October 2016; revised 9 February 2017; accepted 13 February 2017; published online 23 February 2017.

*For correspondence (e-mail huixia@zju.edu.cn).

†W.Y. and Y.Y. contributed equally to this study.

‡Present address: College of Resources and Environment, Huazhong Agricultural University, Wuhan 430070, China.

SUMMARY

Inorganic phosphate (Pi) transporters (PTs) play vital roles in Pi uptake and translocation in plants. Under Pi sufficient conditions, PTs are degraded to prevent excess Pi accumulation. The mechanisms targeting PTs for degradation are not fully elucidated. In this study, we found that the *Oryza sativa* (rice) ortholog of *Arabidopsis thaliana* nitrogen limitation adaptation (NLA), OsNLA1 protein, a RING-type E3 ubiquitin-ligase, was predominantly localized in the plasma membrane, and could interact with rice phosphate transporters OsPT2 and OsPT8. Mutation of the 265th cysteine residue in OsNLA1 that was required for ubiquitination prevented breakdown of OsPT2/PT8, suggesting OsNLA1 targeted OsPT2/PT8 for degradation. Mutation in *OsNLA1* (*osnla1*) led to a significant increase of Pi concentration in leaves in a nitrate-independent manner. Overexpression of *OsNLA1* or repression of *OsPT2*/*PT8* restored the high leaf Pi concentration in *osnla1* mutants to a level similar to that of wild-type plants. In contrast to what has been observed in Arabidopsis, the transcript abundance of *OsNLA1* did not decrease under Pi limited conditions or in *OsmiR827* (microRNA827)- or *OsPHR2* (PHOSPHATE STARVATION RESPONSE 2)-overexpressing transgenic lines. Moreover, there was no interaction of OsNLA1 and OsPHO2, an E2 ubiquitin-conjugase, suggesting that OsPHO2 was not the partner of OsNLA1 involved in ubiquitin-mediated PT degradation. Our results show that OsNLA1 is involved in maintaining phosphate homeostasis in rice by mediating the degradation of OsPT2 and OsPT8, and OsNLA1 differs from the ortholog in Arabidopsis in several aspects.

Keywords: *Oryza sativa*, phosphate transporter, nitrogen limition adaptation, an ubiquitin ligase with SPX domain, ubiquitination, PHO2, an ubiquitin-conjugating enzyme.

INTRODUCTION

Phosphorus (P) is an essential and often limiting macronutrient for plant growth and development. As plants take up P exclusively in the form of inorganic phosphate (Pi), high immobilization rates of Pi in soil, slow diffusion and substantial fractions of organically bound P result in limited Pi for plants in soil (Bieleski, 1973). Plants have evolved a variety of strategies to enable growth in limited Pi soils, including alteration of root structure to accelerate soil exploration, metabolic changes to maintain intracellular Pi homeostasis, and induction and secretion of phosphatases and organic acids to mobilize Pi from organic matters (Vance *et al.*, 2003; Tran *et al.*, 2010; Wu *et al.*, 2013; Peret *et al.*, 2014).

Genes encoding plant phosphate transporter (PT) comprise a large family with important roles in various physiological and development processes (Javot *et al.*, 2007; Liu *et al.*, 2011). Plants exploit both high- and low-affinity Pi transporters. The former type of Pi transporters are induced by limited Pi and operate at Pi concentration in the micromolar range, whereas the latter ones are constitutively expressed and absorb Pi at millimolar concentrations (Ai *et al.*, 2009; Jia *et al.*, 2011). The Pi transporters are

classified into five families based on their subcellular locations: the PHT1 family is localized in the plasma membrane (PM), PHT2 family in plastids, PHT3 family in mitochondria, PHT4 family in Golgi, and PHT5 family in vacuoles (Guo *et al.*, 2008; Nussaume *et al.*, 2011; Wang *et al.*, 2015; Liu *et al.*, 2016). The majority of plant Pi transporters belong to PHT1 family, which are homologs of the yeast (*Saccharomyces cerevisiae*) Pho84 Pi transporter, and belong to the major facilitator superfamily (Javot *et al.*, 2007). There are nine and 13 PTs belonging to the PHT1 family in *Arabidopsis thaliana* and *Oryza sativa* (rice), respectively. Analysis of the PHT1 family in rice revealed a variety of expression patterns, consistent with a large functional range of the family in Pi transport (Liu *et al.*, 2011; Nussaume *et al.*, 2011). OsPT2 has been found to be a low-affinity Pi transporter that is responsible for Pi transport from root to shoot in rice (Ai *et al.*, 2009). OsPT8 is a high-affinity transporter, which is involved in uptake and transfer of Pi from vegetative organs to reproductive organs (Liu *et al.*, 2011). Besides the regulation at the RNA level, post-translational regulation also plays an important role in the activity of Pi transporters. For instance, under Pi sufficient conditions, rice casein kinase II (CK2) can phosphorylate PTs, thereby inhibiting the interaction between PTs and PHOSPHATE TRANSPORTER TRAFFIC FACILITATOR 1 (PHF1) responsible for assisting the trafficking of PTs from the endoplasmic reticulum (ER) to the PM, resulting in ER retention of PTs. Under Pi limiting conditions, CK2 is degraded and PHF1 facilitates the trafficking of non-phosphorylated PTs from the ER to the PM where they function (Chen *et al.*, 2011, 2015).

NITROGEN LIMITION ADAPTATION (NLA) was first cloned from an Arabidopsis mutant that failed to develop the essential adaptive responses to nitrate limitation and displayed early senescence (Peng *et al.*, 2007). It is also involved in accumulation of salicylic acid and immune responses (Yaeno and Iba, 2008). The NLA protein comprises a N-terminal SPX domain (Pfam PF03105), which is named after the Suppressor of Yeast G-protein a-subunit1 (SYG1), the yeast Phosphatase81 (PHO81), and the human Xenotropic and Polytrophic Retrovirus receptor1 (XPR1), and a C-terminal RING domain responsible for putative ubiquitin E3 ligase activity (Guerra and Callis, 2012). SPX domain-containing proteins have been shown to play important roles in a broad variety of processes involved in Pi homeostasis in yeast (Secco *et al.*, 2012) and plants, such as Pi transport, signaling and remobilization (Hamburger *et al.*, 2002; Wang *et al.*, 2009, 2014, 2015; Lv *et al.*, 2014). Arabidopsis NLA has been demonstrated to mediate the degradation of PHT1s in the PM. Under Pi deficiency, the Arabidopsis microRNA (miR827) is induced and mediates the post-transcriptional cleavage of *NLA* mRNA to increase the abundance of PHT1s in PM to accelerate Pi uptake (Kant *et al.*, 2011; Lin *et al.*, 2013). Also, in Arabidopsis *nla* mutant, the increased abundance of PHT1s in PM led to high leaf Pi content under Pi sufficient conditions (Lin *et al.*, 2013).

The Arabidopsis *pho2* mutant defective in an ubiquitin-conjugating E2 enzyme was identified as a Pi over-accumulator from an ethyl methylsulfonate mutagenesis library screen (Aung *et al.*, 2006; Bari *et al.*, 2006). PHO2 mediates the degradation of PHF1 protein that is involved in facilitating the trafficking of AtPHTs from the ER to the PM (Gonzalez *et al.*, 2005; Huang *et al.*, 2013). PHO2 also mediates the degradation of PHO1 protein (Liu *et al.*, 2012) that is responsible for loading Pi from root to shoot via xylem (Hamburger *et al.*, 2002; Stefanovic *et al.*, 2011), and PHT1;1 and PHT1;4 (Huang *et al.*, 2013; Park *et al.*, 2014), which are the major Pi transporters under both Pi sufficient and Pi limited conditions (Shin *et al.*, 2004; Peng *et al.*, 2007). *PHO2* is the target of miR399, which mediates post-transcriptional cleavages of *PHO2* mRNA upon Pi deficiency. It has been shown that in Arabidopsis upon Pi starvation, NLA and PHO2 cooperatively degrade Pi transporters through an integration of microRNA-mediated post-transcriptional and ubiquitin-mediated post-translational pathways (Huang *et al.*, 2013; Lin *et al.*, 2013).

In comparison with Arabidopsis, the knowledge about the function of the orthologs of the *NLA* gene in monocot crops is limited. In this study, we show that in rice OsNLA1 protein can interact with OsPT2 and OsPT8 to mediate their degradation. Inactivation of Os*NLA1* by mutation leads to the Pi over-accumulation phenotype in a nitrate-independent manner. Either overexpression of *OsNLA1* or repression of *OsPT2* or *OsPT8* by RNA interference in the *osnla1* mutant background restores Pi concentration to normal levels. In contrast to the Arabidopsis ortholog, the transcript abundance of *OsNLA1* did not change in response to Pi limitation, and also no changes were observed in *OsmiR827* or *OsPHR2*-overexpressing lines. No interaction between OsNLA1 and OsPHO2 was observed. Our results demonstrated that OsNLA1 differs from its ortholog in Arabidopsis in several aspects.

RESULTS

OsNLA1 is a PM protein

Previously, we identified two orthologs of Arabidopsis *NLA* (*AtNLA*) in rice, named Os*NLA1* and *OsNLA2* (Secco *et al.*, 2012). Like AtNLA, OsNLA1 and OsNLA2 contained a N-terminal SPX domain and a C-terminal RING domain (Figure S1). Protein alignment revealed that OsNLA1 and OsNLA2 show 60% and 41% sequence identity with NLA, respectively (Figure S1). The subcellular localizations of OsNLA1 and OsNLA2 proteins were determined in rice protoplasts. The coding sequences of *OsNLA1* and *OsNLA*2 were fused to N-terminus of mCherry, and transiently expressed in rice protoplasts using a PEG-meditated

transformation system. The strong mCherry signals in the PM of rice protoplasts were observed for OsNLA1 (Figure 1a). To verify the subcellular localization, transient expression of OsNLA1-GFP was carried out in tobacco leaves using Agrobacterium-mediated infiltration. OsNLA1 was predominantly localized in the PM (Figure 1b), which is similar to its Arabidopsis counterpart (Lin *et al.*, 2013). OsNLA2 showed no specific subcellular localization in both rice protoplasts and tobacco leaves (Figure 1a and b). Soluble and membrane protein fractions were extracted separately from tobacco leaves transiently expressing the *3FLAG-OsNLA1* or *3FLAG-OsNLA2* fusion protein. Immunoblotting analysis with anti-FLAG antibody showed that OsNLA1 was detected in the membrane fraction, but not in the soluble fraction, whereas OsNLA2 was detected in both soluble and membrane fractions (Figure 1c). The H^+-ATPase was used as a membrane protein control (Elmore and Coaker, 2011). Based on the PM localization of the OsNLA1, the research was focused on OsNLA1 to investigate its role in maintaining Pi homeostasis.

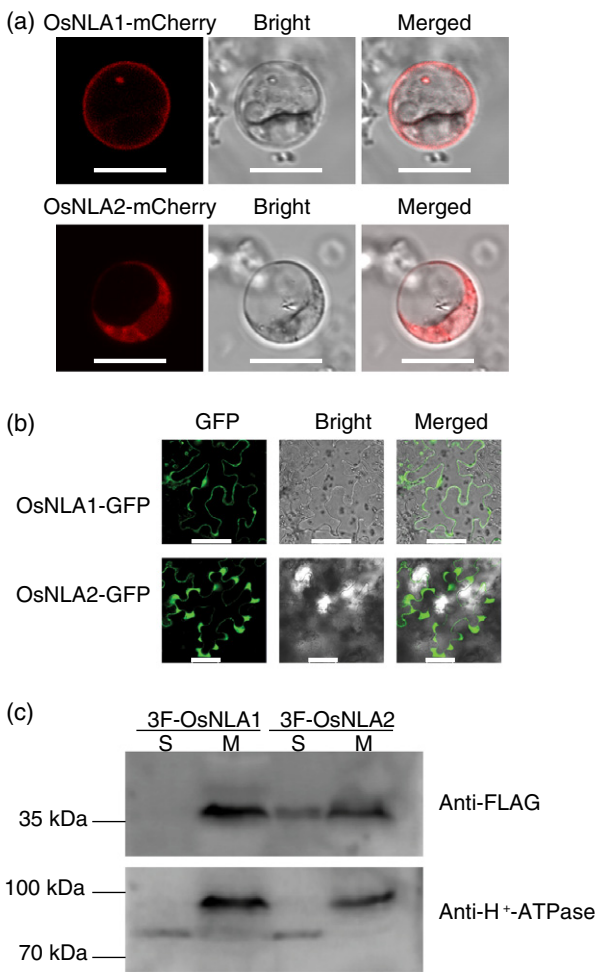

Figure 1. OsNLA1 is localized to the plasma membrane (PM).
(a) Subcellular localization of OsNLA1/2-mCherry in rice protoplasts. Scale bars: 10 μm.
(b) Subcellular localization of OsNLA1/2-GFP in tobacco leaves via Agrobacterium-mediated infiltration. Scale bars: 50 μm. For (a) and (b), the fluorescence signal was detected with a confocal laser-scanning microscope.
(c) Immunoblot analyses of OsNLA1/2 in soluble and membrane protein fraction extracted from tobacco leaves transformed with *3FLAG-OsNLA1* or *3FLAG-OsNLA2*. Anti-FLAG and anti-H^+-ATPase antibodies were used to detect OsNLA1/2 and H^+-ATPase (a membrane protein marker), respectively. M, membrane protein fraction; S, soluble protein fraction.

Mutation in *OsNLA1* led to significant increase of leaf Pi concentration in a nitrate-independent manner

To investigate the function of OsNLA1, two mutants, *osnla1-1* and *osnla1-2*, were obtained from the rice *TOS17* transposon insertion library (https://tos.nias.affrc.go.jp/). The *TOS17* transposon was inserted into the second intron and third exon of *OsNLA1* gene in *osnla1-1* and *osnla1-2*, respectively (Figure 2a). Homozygous *osnla1* mutants were confirmed by polymerase chain reaction (PCR; Figure S2). Transgenic plants overexpressing *OsNLA1* coding sequence (CDS) under the control of the *Cauliflower mosaic virus* (CaMV) 35S promoter were generated in the wild-type (WT) Nipponbare (NIP) background. Quantitative reverse transcription (qRT)-PCR and reverse transcription (RT)-PCR were carried out to examine the transcript abundance of *OsNLA1* in both *osnla1* mutants and *OsNLA1*-overexpressing (OE) transgenic lines under Pi sufficient condition. The *OsNLA1* transcript abundance was reduced to 25–35% in *osnla1-1* compared with that of the NIP, and completely abolished in *osnla1-2* (Figure 2a). Overexpression of *OsNLA1* resulted in a significant increase in transcript abundance in two independent transgenic lines (Figure 2b).

Arabidopsis *nla* mutants had a significant increase in leaf Pi concentration compared with the WT (Kant *et al.*, 2011). To investigate the effect of OsNLA1 on Pi homeostasis in rice, the growth performance and the leaf and root Pi concentrations of the *osnla1*, *OsNLA1*-OE transgenic plants and WT plants grown under Pi sufficient or Pi limited conditions were examined. Under both Pi sufficient and deficient conditions, no significant difference in plant growth among the *OsNLA1*-OE transgenic lines, *osnla1* mutants and the WT were observed (Figure S3a). Under Pi sufficient conditions, necrotic symptoms were observed in mature leaf tips of both the *osnla1* mutants (Figure 2c). The Pi concentrations in all the detected leaves, from the 3rd to 7th (designed from old to young), of the *osnla1-1* and *osnla1-2* mutants were more than four times higher than those of the WT grown under Pi sufficient conditions, which is statistically significant (Figure 2d). For the *OsNLA1*-OE transgenic lines, no significant differences in leaf Pi concentrations were found, except those of the 5th leaf in *OsNLA1*-OE1 and the 7th leaf in *OsNLA1*-OE2 (Figure 2d). Under Pi deficient conditions, no Pi excessive toxicity was observed in mature leaves of both *osnla1* mutants;

however, increased Pi concentration was observed in the 3rd and 4th leaf of *osnla1-2* compared with the WT (Figure 2d). The biomass and the relative expression of several phosphate starvation-induced (PSI) genes were also examined. The reduced shoot biomass, increased root/shoot biomass ratio of all material and induced PSI genes, *OsmiR399d* (microRNA399), *OsSPX1*, *OsSQD* (sulfoquinovosyldiacylglycerol 2), *OsPAP10a* (purple acid phosphatase 10) and *OsIPS1* (induced by phosphate starvation 1), in roots of WT were observed when grown under Pi deficient conditions (Figure S3b and c).

To confirm the high leaf Pi concentration in *osnla1* is directly caused by the mutation of *OsNLA1* gene, the *osnla1*-2 mutant was complemented with the *OsNLA1*-OE construct using the CaMV 35S promoter. Two complementary transgenic lines were confirmed by qRT-PCR, and the leaf Pi concentration in both complemented lines was greatly reduced under Pi sufficient conditions (Figure 2e).

It has been reported that NLA regulates Pi homeostasis in a nitrate-dependent manner in Arabidopsis (Kant *et al.*, 2011). Arabidopsis *nla* mutant grown under low NO_3^- conditions can accumulate six times higher Pi content in leaves than that grown under high NO_3^- conditions (Kant *et al.*, 2011). To examine whether the nitrate supply affects the function of OsNLA1 in rice, the leaf Pi content of *osnla1* mutants supplied with different combinations of Pi and NO_3^- concentrations were examined. Considering that the nutrient solution used in the soil experiment of Arabidopsis *nla* mutant to elucidate the function of NLA in a nitrate-dependent manner contained about 30 times Pi and seven times NO_3^- concentration of that used in our hydroponic solution, we also added high Pi (HP; five times) and high NO_3^- (HN; five times) into combinations to treat plants. No different growth performances were observed when both *osnla1* mutants and WT were grown under −P condition (0.016 mM) regardless of the levels of nitrate supplies, which was consistent with no significant change of leaf Pi concentration (Figure 2g). When grown under +P (0.323 mM) conditions regardless of the levels of nitrate supplies, the leaf Pi concentrations of both *osnla1* mutants were four times that of WT, and the mature leaf tips of both *osnla1* mutants showed necrotic symptoms (Figure 2f and g). When grown under HP (1.615 mM) conditions regardless of the levels of nitrate supplies, the mature leaf tips of both *osnla1* mutants showed more severe necrotic symptoms than those under +P conditions, and the leaf Pi concentration of both *osnla1* mutants were twice that of WT, which already showed phosphate toxicity in mature leaf tips because of high Pi concentration (Figure 2f and g). The reduced shoot biomass and increased root/shoot biomass ratio of *osnla1* mutants and WT were observed under −P conditions, and also the PSI genes (*OsIPS1* and *OsSPX1*) and nitrate starvation response genes, *OsNAR2.1* (nitrate transport accessory protein 2.1) and *OsNRT2.1* (nitrate transporter 2.1), in roots of WT were upregulated under Pi deficient and NO_3^- deficient conditions, respectively (Figure S3e and g). Thus, *osnla1* mutants accumulate Pi in a nitrate-independent manner, differing from the findings in Arabidopsis (Kant *et al.*, 2011).

OsNLA1 is not regulated by OsPHR2 and *OsmiR827* at transcriptional level

The PHR1-binding site (P1BS) is the target site of the central transcription factor PHR in both Arabidopsis and rice (Zhou *et al.*, 2008; Bustos *et al.*, 2010; Wu *et al.*, 2013). No P1BS sequence was found in the 2-kb promoter region of the Os*NLA1* gene. To determine whether *OsNLA1* is regulated by the OsPHR2, the transcript abundance of Os*NLA1* was determined in Os*PHR2*-OE transgenic plants under both Pi sufficient and Pi limited conditions (Figure S4; Zhou *et al.*, 2008). *OsNLA1* transcript abundance showed no significant changes in response to Pi starvation stress or overexpression of *OsPHR2*, indicating that the expression of *OsNLA1* is not directly regulated by the OsPHR2-mediated Pi starvation signaling pathway (Figure 3).

NLA was reported to be a target of *miR827* that acts in the Pi starvation response in Arabidopsis (Kant *et al.*, 2011). The transcript abundance of *NLA* is downregulated upon Pi limitation (Kant *et al.*, 2011). Unlike *AtNLA*, there is no *OsmiR827* target sequence in *OsNLA1* sequence. The transcript abundance of *OsNLA1* in *OsmiR827*-OE plants (Figure S4) was similar to that in the WT (Figure 3), indicating that *OsNLA1* is not regulated by OsmiR827-involved pathway in rice.

OsNLA1 interacts with OsPT2 and OsPT8 via the SPX domain

AtNLA was shown to regulate the degradation of PHT1s (Lin *et al.*, 2013). To investigate the effect of OsNLA1 on Pi transporters in rice, the transcript abundance of the two major rice PTs, including the low-affinity Pi transporter OsPT2 and the high-affinity Pi transporter OsPT8, was determined in *osnla1-2* under Pi sufficient conditions. No significant difference was found in the transcriptional abundance of Os*PT2* or Os*PT8* in *osnla1-2* (Figure 4a), suggesting that they are not regulated by OsNLA1 at the transcript abundance level. To investigate whether OsPT2 and OsPT8 are regulated by OsNLA1 at the protein level, bimolecular fluorescence complementation (BiFC) assays of N-terminal of yellow fluorescence protein (nYFP) fused to OsNLA1 with C-terminal YFP (cYFP) fused to OsPT2 or OsPT8 were carried out in tobacco leaves. No YFP signal was detected in the combination of OsNLA1-nYFP with OsPT2-cYFP or OsPT8-cYFP (Figure 4b). To exclude the possibility that OsPT2 or OsPT8 were ubiquitinated via OsNLA1 and then degraded, the 265th cysteine residue in the RING domain of the OsNLA1, which is conserved with

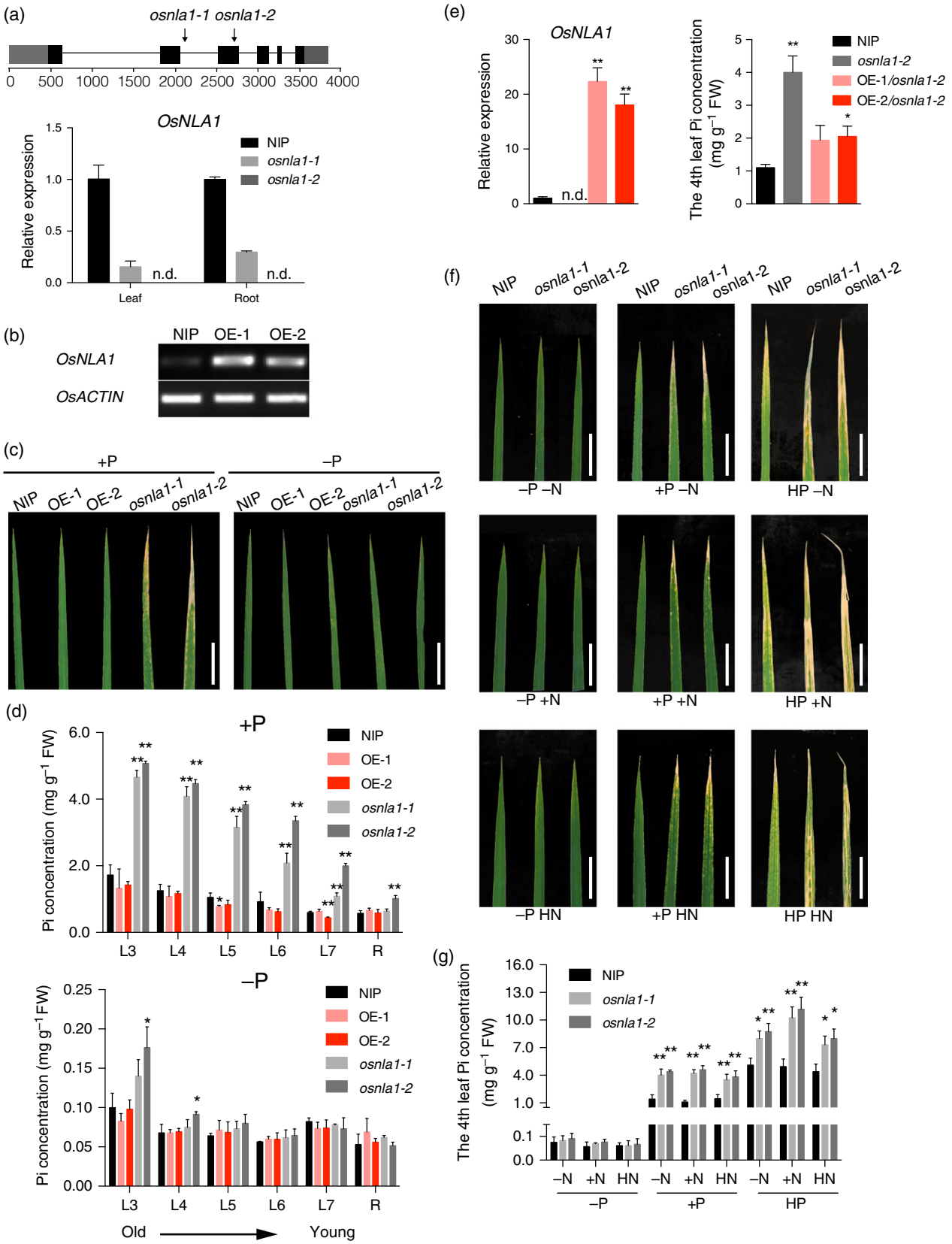

Figure 2. High leaf inorganic phosphate (Pi) concentration of *osnla1* mutant is nitrate-independent.
(a) Characterization of *TOS17* insertion *osnla1* mutants. Untranslated regions, exons and introns are shown with gray boxes, black boxes and black lines, respectively. Black arrows show *TOS17* insertion sites. For the quantitative reverse transcription-polymerase chain reaction (qRT-PCR) analysis, plants were grown under Pi sufficient conditions for 3 weeks.
(b) RT-PCR analysis of *OsNLA1* transcript abundance in two *OsNLA1*-overexpressing (OE) transgenic lines. Plants were grown under Pi sufficient conditions for 3 weeks. *OsACTIN* was used as a control.
(c and d) Enlarged images of mature leaf tips (c) and Pi concentration (d) of 3rd to 7th leaf and root of *osnla1* mutants, *OsNLA1*-OE transgenic lines and wild-type (NIP) plants. Plants were grown under Pi sufficient conditions (+P, 0.323 mM Pi) for 7 days, and then transferred to Pi sufficient or Pi deficient conditions (−P, 0.016 mM Pi) for another 14 days. Scale bars: 1 cm. L3–L7 and R represent the 3rd to 7th leaf from old to young and root, respectively.
(e) The relative expression of *OsNLA1* and the Pi concentration of the 4th leaf in NIP, *osnla1-2* and two *osnla1-2* complementary lines (OE-1/*osnla1-2* and OE-2/*osnla1-2*). Plants were grown under Pi sufficient conditions for 3 weeks.
(f and g) Enlarged images of mature tips (f) and the 4th leaf Pi concentration (g) of *osnla1* mutants and NIP under different combinations of Pi and NO_3^- concentrations. Plants were grown under phosphate and nitrate sufficient (+P+N) conditions for 7 days, and then transferred to −P−N, −P+N, −PHN, +P−N, +P+N, +PHN, HP−N, HP+N and HPHN conditions, respectively, for another 14 days. Scale bars: 1 cm.
For (d), (e) and (g), data represent means + SD ($n = 3$). Student's *t*-test was used to determine the significant difference from that of the corresponding NIP in each treatment. *P*-values <0.05 and <0.01 are indicated with * and **, respectively.
FW, fresh weight; NIP, wild-type Nipponbare. The different phosphate and nitrate concentrations are indicated as: −P, 0.016 mM Pi; +P, 0.323 mM Pi; HP, 1.615 mM Pi; −N, 0.427 mM NO_3^-; +N, 1.425 mM NO_3^-; HN, 7.125 mM NO_3^-.

the cysteine in AtNLA responsible for ubiquitination, was mutated into alanine (Lin *et al.*, 2013). YFP fluorescence signal was visualized for complementation assay of OsNLA1^{C265A}-nYFP with OsPT2-cYFP or OsPT8-cYFP in the PM in tobacco leaves, whereas no YFP signal was detected in the negative control of co-expression of OsNLA1^{C265A}-nYFP and OsIRT1-cYFP (Figure 4b). The YFP signal from the BiFC coincided to the signal from the PM marker of Arabidopsis PM intrinsic protein 2A fused to mCherry (AtPIP2A-mCherry; Prak *et al.*, 2008). To further verify the degradation of OsPT2 or OsPT8 by OsNLA1, the OsPT2 and OsPT8 protein levels were examined in the membrane protein fraction extracted from *4MYC-OsPT2* or *4MYC-OsPT8* transiently transformed tobacco leaves with or without *3FLAG-OsNLA1*. The result showed OsNLA1 can significantly reduce the OsPT2 or OsPT8 protein abundance (Figure 4c and d).

The SPX domain has been reported to be responsible for protein–protein interaction in yeast and plants (Hurlimann *et al.*, 2009; Lv *et al.*, 2014; Wang *et al.*, 2014). To examine whether OsNLA1 interacts with OsPT2 or OsPT8 via the SPX domain, the OsNLA1 protein was divided into N-terminal SPX domain (OsNLA^{SPX}) and C-terminal RING domain (OsNLA1^{RINGC265A}; Figure S1). When OsNLA1^{SPX}-nYFP was co-expressed with OsPT2/OsPT8-cYFP in tobacco leaves, YFP signal can be detected, whereas no YFP signal was observed for co-expression of OsNLA1^{RINGC265A}-nYFP and OsPT2/OsPT8-cYFP, suggesting that OsNLA1 interacts with OsPT2 and OsPT8 via the SPX domain (Figure 5). Some RING type E3 ligases were reported to function as a dimer (Xie *et al.*, 2002; Dou *et al.*, 2012). The YFP signals was observed in the PM of tobacco leaves that co-expressed OsNLA1^{C265A}-nYFP and OsNLA1^{C265A}-cYFP, suggesting OsNLA1 functions as a dimer (Figure 5).

OsNLA1 affects phosphate homeostasis via OsPT2 and OsPT8 in rice

To provide genetic evidence of regulation of OsPT2 and OsPT8 by OsNLA1, OsPT2 and OsPT8 RNA interference (Ri) constructs were transformed into the *osnla1-2* mutant. Two transgenic lines, *OsPT2*-Ri/*osnla1-2* and *OsPT8*-Ri/*osnla1-2* were identified. The qRT-PCR confirmed the decrease in target transcript abundance in the Ri lines (Figure 6a). Analysis of leaf Pi concentrations showed that the reduction of the transcript abundance of *OsPT2* or *OsPT8* in the Ri lines resulted in the decrease of the leaf Pi concentration in *osnla1* mutant to the WT level (Figure 6b). Thus, genetically reducing the amount of *OsPT2* or *OsPT8* suppresses the Pi over-accumulation phenotype of *osnla1* in rice.

Figure 3. *OsNLA1* transcript abundance in *OsPHR2*- and *OsmiR827*-overexpressing (OE) transgenic plants, *osnla1-2* and wild-type (NIP).
Total RNA was extracted from leaves and roots of *OsPHR2*-OE, *OsmiR827*-OE, *osnla1-2* and NIP. Plants were grown under inorganic phosphate (Pi) sufficient (+P) conditions for 14 days, followed by transfer to +P and −P conditions for another 7 days. Data show mean + SD ($n = 3$). Student's *t*-test was used to determine the significance of differences between NIP and *osnla1-2* mutant or transgenic lines.

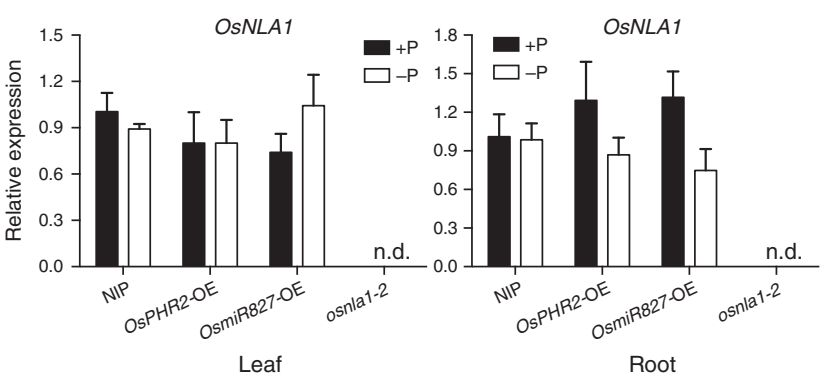

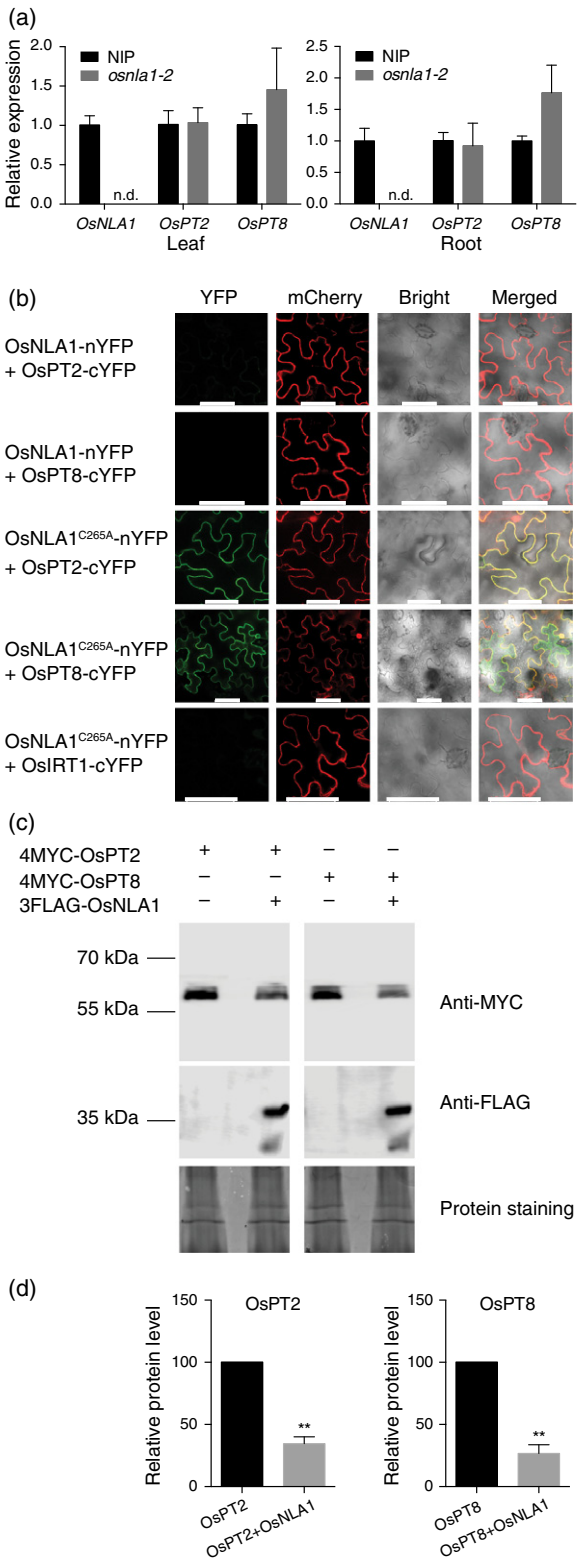

Figure 4. Interaction of OsNLA1 with OsPT2 or OPT8.
(a) Quantitative reverse transcription-polymerase chain reaction (qRT-PCR) of *OsPT2* and *OsPT8* in the wild-type (NIP) and *osnla1-2* plants grown under inorganic phosphate (Pi) sufficient conditions for 3 weeks.
(b) Bimolecular fluorescence complementation (BiFC) analysis to detect *in vivo* interaction between OsNLA1 and OsPT2 or OsPT8 in tobacco leaves. N-terminal fragments of YFP (nYFP) were fused to C-terminus of OsNLA1 (OsNLA1-nYFP) and mutated version of OsNLA1 (OsNLA1^{C265A}-nYFP), and C-terminal fragments of YFP (cYFP) were fused to C-terminus of OsPT2 or OsPT8 (OsPT2-cYFP or OsPT8-cYFP). AtPIP2A-mCherry was used as a plasma membrane (PM) protein marker. OsIRT1-cYFP with OsNLA1 construct was used as negative control. Scale bars: 50 μm.
(c) OsPT2 or OsPT8 is degraded by OsNLA1 in tobacco leaves. Membrane proteins were extracted from *4MYC-OsPT2* or *4MYC-OsPT8* transformed tobacco leaves with or without *3FLAG-OsNLA1*. Anti-MYC and anti-FLAG antibodies were used to detect OsPT2/8 and OsNLA1, respectively.
(d) Quantification of the results shown in (c). Relative OsPT2/PT8 protein level is the ratio of the OsPT2/PT8 protein in tobacco transformed with *4MYC-OsPT2*/*PT8* and *3FLAG-OsNLA1* to that transformed with *4MYC-OsPT2*/*PT8* alone. Data represent means + SD ($n = 3$). Data significantly different from the corresponding controls are indicated (**$P < 0.01$; Student's *t*-test).

OsNLA1 does not interact with OsPHO2

OsPHO2 contains an UBC domain that is responsible for activity of the E2 ubiquitin- conjugating enzyme and *ospho2* mutant contains high Pi concentration in leaves (Cao *et al.*, 2014). Also, it has been shown that NLA and PHO2 cooperatively regulate Pi transporters through ubiquitin-mediated degradation in Arabidopsis (Huang *et al.*, 2013; Lin *et al.*, 2013). We first speculated that OsPHO2 may interact with OsNLA1 to regulate OsPTs. To test the hypothesis, a BiFC assay of OsNLA1^{C265A}-nYFP and OsPHO2-cYFP was carried out. No YFP signal was detected (Figure S5). The 748th cysteine of the UBC domain of AtPHO2 has been shown to be important for mediating the degradation of PHO1. Mutation of the cysteine into alanine, PHO2^{C748A}, can prevent the sequential degradation of PHO1 (Liu *et al.*, 2012). To avoid the possibility of degradation of OsNLA1, the 719th cysteine in OsPHO2, which is corresponding to the 748th cysteine in AtPHO2, was replaced by alanine. The resulting OsPHO2^{C719A}-cYFP was co-expressed with OsNLA1^{C265A}-nYFP, and no restored YFP signal was observed. Taken together, it suggested that OsNLA1 may mediate the degradation of OsPT2 and OsPT8 with an ubiquitin-conjugating E2 enzyme other than OsPHO2.

DISCUSSION

Plants have evolved complex regulatory networks to cope with low levels of Pi in soil. While these approaches optimize the acquisition of Pi to facilitate plant growth, there appears to be a number of negative feedback loops to prevent the excess accumulation of Pi that has detrimental consequences. In this study, we provide several lines of evidence to demonstrate that OsNLA1 mediates the degradation of OsPT2 and OsPT8 to maintain Pi homeostasis in rice. Firstly, OsNLA1 and OsPT2/8 were predominantly co-localized in the PM (Figure 1), which suggests the possibility of their interaction with each other. Secondly, we showed that the interaction between OsNLA1 and OsPT2/8

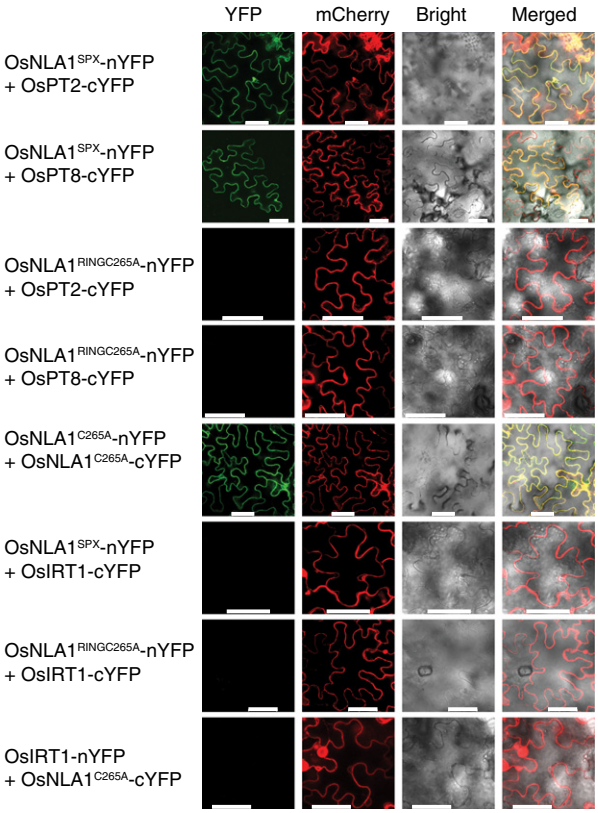

Figure 5. OsNLA1 interacts with OsPT2 or OsPT8 via the SPX domain and forms a dimer.
Bimolecular fluorescence complementation (BiFC) analysis to detect *in vivo* interaction was carried out. N-terminal fragments of YFP (nYFP) were fused to C-terminus of OsNLA1^{SPX}, OsNLA1^{RINGC265A} and mutant OsNLA1^{C265A} (OsNLA1^{SPX}-nYFP, OsNLA1^{RINGC265A}-nYFP and OsNLA1^{C265A}-nYFP), and C-terminal fragments of YFP (cYFP) were fused to C-terminus of OsPT2, OsPT8 and mutant OsNLA1^{C265A} (OsPT2-cYFP, OsPT8-cYFP and OsNLA1^{C265A}-cYFP). AtPIP2A-mCherry was used as a plasma membrane (PM) protein marker indicated by red signals. OsIRT1-nYFP with corresponding OsNLA1 constructs were used as negative control. Scale bars: 50 μm.

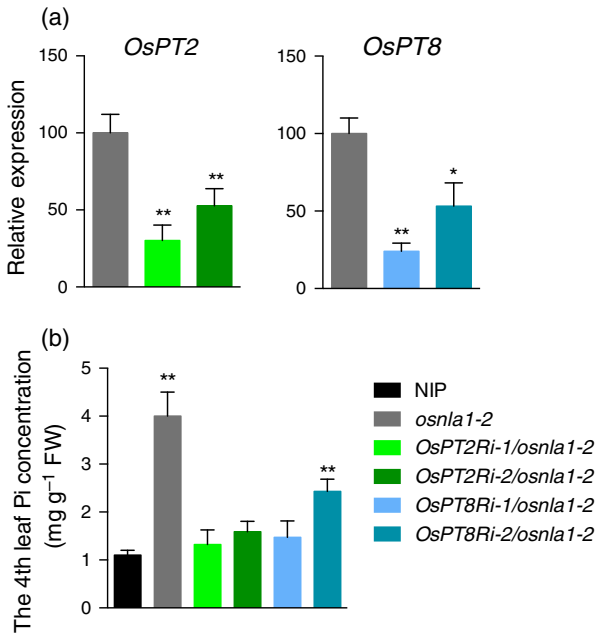

Figure 6. Restoration of the high leaf inorganic phosphate (Pi) concentration of *osnla1-2* by repression of *OsPT2* or *OsPT8*.
(a) Quantitative reverse transcription-polymerase chain reaction (qRT-PCR) detection of *OsPT2* and *OsPT8* RNA interference (Ri) effects in the *osnla1-2* background transgenic plants.
(b) The 4th leaf Pi concentration of wild-type (NIP), *osnla1-2* and transgenic plants. The corresponding transgenic lines are indicated as *OsPT2*Ri-1/*osnla1-2*, *OsPT2*Ri-2/*osnla1-2*, *OsPT8*Ri-1/*osnla1-2* and *OsPT8*Ri-2/*osnla1-2*, respectively.
Plants were grown under Pi sufficient conditions for 3 weeks. [Colour figure can be viewed at wileyonlinelibrary.com]

resulted in the degradation of OsPT2 and OsPT8 (Figure 4b–d). Finally, these conclusions were supported by genetic evidence. While mutation of *OsNLA1* led to Pi over-accumulation, repression of *OsPT2* or *OsPT8* greatly reduced the high leaf Pi concentration in *osnla1-2* (Figures 2e and 6).

The function of NLA to mediate the degradation of Pi transporters is conserved between Arabidopsis and rice. However, under +P conditions and HP conditions (five times), the low NO_3^- (0.3 times) and high NO_3^- (five times) had no effects on leaf Pi concentration of both *osnla1* mutants (Figures 2 and S3). This indicates that OsNLA1 maintains Pi homeostasis in a nitrate-independent manner in rice, whereas AtNLA acts in a nitrate-dependent manner (Kant *et al.*, 2011). Nutrient mobility may account for the fact that on one hand nutrient solution containing 10 mM Pi and 10 mM NO_3^- was best for Arabidopsis growth in soil in a previous report (Kant *et al.*, 2011), and on the other hand the high Pi conditions (1.615 mM Pi, five times) caused necrotic symptoms in mature leaf tips of WT in our hydroponic experiment. Meanwhile, the Pi concentrations in *OsNLA1*-OE transgenic lines were similar to that of the WT (Figure 2d). It is possible that the activity of OsNLA1 is controlled at the translational or post-translational level. In addition, because the ubiquitin-conjugating E2 enzyme (currently unknown) that functions with OsNLA1 to mediate the degradation of OsPT2 and OsPT8 maintains at normal levels in these transgenic lines, the excess OsNLA1 alone might not affect the protein abundance of OsPT2 and OsPT8.

In Arabidopsis, the ubiquitin-E2 conjugating enzyme *PHO2* and the ubiquitin-E3 ligase *NLA* are targets of miR399 and miR827, respectively. Upon Pi starvation, AtNLA and AtPHO2 cooperatively regulate Pi transporters through an integration of microRNA-mediated post-transcriptional and ubiquitin-mediated post-translational regulatory pathways (Huang *et al.*, 2013; Lin *et al.*, 2013; Figure 7). Neither the miR827 target sequence nor the P1BS sequence for PHR2 binding was found in the promoter and genomic sequence of Os*NLA1*. The *OsNLA1* transcript abundance was not altered in *OsmiR827*- and

OsPHR2-OE transgenic lines (Figure 3). Also *OsNLA1* did not respond to Pi limited conditions at the transcript abundance level (Figure 3), differing from *AtNLA*, which decreased in abundance upon Pi limitation (Kant *et al.*, 2011). Thus, while the function of NLA is conserved between Arabidopsis and rice to degrade PHT1 family members, the regulatory network controlling *OsNLA1* abundance differs between Arabidopsis and rice. In Arabidopsis, *NLA1* transcript can be negatively regulated by the central transcription factor PHR1 via its downstream miR827. The negative feedback loop does not operate for the regulation of *OsNLA1* in rice (Figure 7).

In Arabidopsis, it is not clear whether NLA1 and PHO2 work together to ubiquitinate PTs to maintain Pi homeostasis (Lin *et al.*, 2013; Park *et al.*, 2014). Our data showed that OsNLA1 does not interact with OsPHO2 (Figure S5). The OsNLA1-mediated degradation of OsPT2 and OsPT8 requires additional unknown E2 conjugating enzyme. Identification of the E2 via yeast-two-hybrid library screening or a new proteomic approach will be essential for understanding the regulatory network to maintain Pi homeostasis in plants.

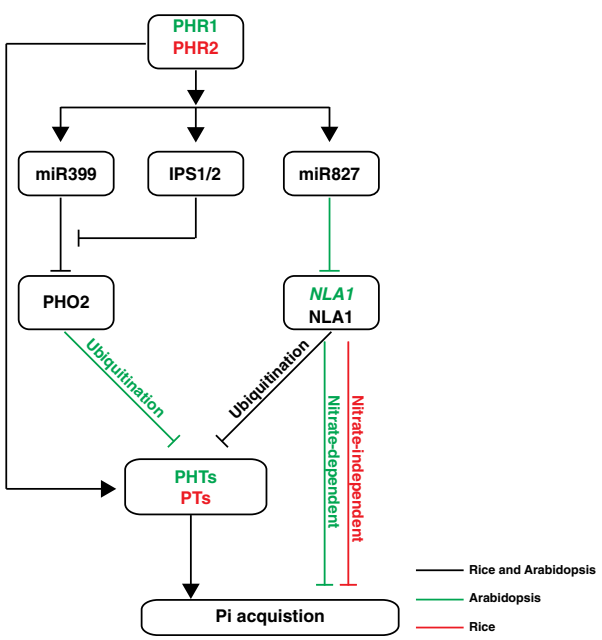

Figure 7. Diagrammatic representation of the role and regulation of NLA in Arabidopsis and rice.
Conserved features between rice and Arabidopsis of NLA are shown with black lines. Arabidopsis-specific features are shown in green, and rice-specific features are shown in red. In brief, miR399, miR827 and IPS1/2 are regulated by key inorganic phosphate (Pi) starvation transcription factor PHR1 (Arabidopsis) or PHR2 (rice). In Arabidopsis, NLA1 and PHO2 cooperatively regulate Pi transporters abundance through an ubiquitin-mediated regulatory pathway, with the abundance of *NLA* negatively regulated by PHR1 and miR827. In contrast, Os*NLA1* is not regulated by PHR2 or miR827 at the transcript abundance level. Furthermore, OsNLA1 acts in a nitrate-independent manner in contrast to AtNLA that acts in a nitrate-dependent manner. Positive and negative effects are indicated by arrows and flat-ended lines, respectively.

In summary, the function of NLA in maintaining phosphate homeostasis via degradation of Pi transporters is conserved between rice and Arabidopsis, but the Pi starvation signal pathway regulating *NLA1* differs between Arabidopsis and rice (Figure 7). In contrast to Arabidopsis, Os*NLA1* transcript abundance is not decreased by Pi limitation and not regulated by PHR2 or microRNA. Furthermore, it does not function in a nitrate-dependent manner. Dissection of these regulatory loops is critical in crop species to translate findings in model species to crop species.

EXPERIMENTAL PROCEDURES

Construction of vectors

The open reading frames (ORF) of Os*NLA1/2* and *OsPT2/8* genes were amplified from cDNA of rice (*O. sativa*) leaves, and then cloned into pDONR201 vector (Invitrogen CA, USA). For subcellular localization, the ORFs of *OsNLA1/2* were inserted into the pH7FWG2 vector (Karimi *et al.*, 2002) to obtain OsNLA1/2-GFP constructs using the GATEWAY system. The ORFs of *OsNLA1/2* were inserted into pSAT4A-mCherry-N1 (http://www.bio.purdue.edu/people/faculty/gelvin/nsf/protocols_vectors.htm) to obtain OsNLA1/2-mCherry constructs. For *3FLAG-OsNLA1/2* constructs, the ORFs of *OsNLA1/2* and 3FLAG from pBS-Omega-3FLAG were amplified, assembled by overlapping sequences and inserted into modified pCAMBIA1300 (Wang *et al.*, 2009). For *4MYC-OsPT2/8* constructs, the ORFs of *OsPT2/8* and 4MYC from pBS-Omega-4MYC were amplified, assembled by overlapping sequences and inserted into modified pCAMBIA1300 (Wang *et al.*, 2009). The RNA interference constructs of *OsPT2 and OsPT8* were obtained by subcloning 255 bp or 250 bp into pH7GWIWG2 (I) (Karimi *et al.*, 2002) at both sense and anti-sense orientations, respectively. The resulting vectors were transferred into Agrobacterium strain EHA105 or EHA101 for rice transformation and transient expression in tobacco leaves. The primers used are listed in Table S1.

Preparation of rice protoplast and subcellular localization assay

Rice seeds were germinated on one-half-strength Murashige and Skoog media under light for 7 days at 26°C, and then in the dark for another 7 days. Using a razor blade, the stems and leaves of the seedlings were cut into approximately 0.5-mm strips. The strips were placed into 10 ml of K3 medium containing 1.5% (w/v) cellulose and 0.3% (w/v) macerozyme (Onozuka Yakult Honsha). Vacuum was applied for 1 h for infiltration of the enzyme solution, and incubated for 4 h in the dark with gentle shaking (approximately 40 rpm) at room temperature. The enzyme solution was washed with 10 ml of W5 medium containing 154 mM NaCl, 125 mM $CaCl_2$, 5 mM KCl and 2 mM MES, pH 5.7, with gentle shaking (approximately 80 rpm) three times. The protoplasts were filtered through a 35-μm nylon mesh and collected by centrifuging at 1500 rpm for 4 min.

Constructs for subcellular localization assay were transformed into rice protoplasts by the polyethylene glycol-mediated method. In brief, 10 μg of plasmid DNA of each construct was transformed into 0.2 ml of protoplast suspension. Then, 220 μl of 40% (v/v) polyethylene glycol was added and mixed immediately by gently shaking. The mixture was incubated for 20 min at room temperature, and 1 ml of K3 medium was added. After incubation at 25–30°C in the dark for 13–15 h, fluorescence signals in rice protoplasts were detected using an LSM710nlo confocal laser-scanning

microscope (Zeiss, Jena, Germany). The plasmid AtPIP2A-mCherry was used as a PM control.

BiFC assay

The target genes were cloned into either C-terminal or N-terminal fragments of YFP vectors (Yang *et al.*, 2007). The resulted constructs were transiently expressed in tobacco leaves by Agrobacterium-mediated infiltration (stain EHA105), as described previously (Walter *et al.*, 2004). The YFP fluorescence of tobacco leaves was imaged 3 days after infiltration using a Zeiss LSM710NLO confocal laser-scanning microscope. Excitation/emission wavelengths were 488 nm/506–538 nm for YFP, and 561 nm/575–630 nm for mCherry.

Immunoblotting

For extraction of soluble and membrane protein, the tobacco leaves transformed with functional *3FLAG-OsNLA1*/2 with or without *4MYC-OsPT2/8* were ground in liquid nitrogen and extracted according to the plant fractionated protein extraction kit (PE0240, Sigma, USA) or Proteoprep membrane extraction kit (PROTMEM, Sigma, USA). Protein concentration was determined by the BAC protein assay. Membrane protein (50 μg) of each sample was loaded onto sodium dodecyl sulfate–polyacrylamide gel electrophoresis (SDS–PAGE) gels and transferred to polyvinylidene fluoride membranes using Trans-Blot Turbo Transfer System (Bio-Rad Laboratories, Hercules, CA, USA). The membrane was blocked with TBST (10 mM Tris-Cl, 150 mM NaCl and 0.05% Tween 20, pH 8.0) containing 5% non-fat milk (TBSTM) at room temperature for 60 min, and incubated with primary antibody in TBSTM overnight at 4°C. Membranes were washed with TBST (three times for 5 min each) and then incubated with the appropriate horseradish peroxidase-conjugated secondary antibodies in TBSTM at room temperature for 1.5 h. After washing three times, bound antibodies were visualized with ECL substrate (Millipore) using the ChemDoc XRS system (Bio-Rad). Quantitative analysis of immunoblots was performed by means of Quantity Tools of Image Lab software (Bio-Rad). The dilution for anti-FLAG (Sigma-Aldrich), anti-MYC (Merck) and anti-H^+-ATPse (Agrisera) were 1:3000, 1:2000 and 1:5000, respectively.

Plant material and growth conditions

The *osnla1* mutants (NF5039 and NF0010) were obtained from the rice *Tos17* insertion mutant database (https://tos.nias.affrc.go.jp/). The primers used for homozygosity of *osnla1* mutants are listed in Table S1.

The rice (*O. sativa* L. *japonica*) cv NIP was used for all physiological experiments and rice transformations. Hydroponic experiments were conducted using a modified rice culture solution containing 1.425 mM NH_4NO_3, 0.323 mM NaH_2PO_4, 0.513 mM K_2SO_4, 0.998 mM $CaCl_2$, 1.643 mM $MgSO_4$, 0.25 mM $NaSiO_3$, 0.009 mM $MnCl_2$, 0.075 mM $(NH_4)_6Mo_7O_{24}$, 0.019 mM H_3BO_3, 0.155 mM $CuSO_4$, 0.152 mM ZnSO4 and 0.125 mM EDTA-Fe (II) at pH 5.5 (Wang *et al.*, 2009). The nutrient solution was replaced every 3 days. Rice plants were grown in growth rooms with a 12-h photo-period (200 μmol photons m^{-2} s^{-1}) and a day/night temperature of 30°C/22°C after germination. Humidity was controlled at approximately 60%. For phenotyping and Pi concentration measurement, seeds were germinated and grown for 3 weeks.

For different Pi supply treatments, rice seeds were germinated and grown hydroponically for 7 days with sufficient Pi supply (0.323 mM Pi) and transferred to Pi sufficient or Pi starvation (0.016 mM Pi) solution for 2 weeks prior to sampling.

For different Pi and NO_3^- supply treatments, plants were grown under phosphate and nitrate sufficient (+P+N) condition for 7 days and then transferred to −P−N, −P+N, −PHN, +P−N, +P+N, +PHN, HP−N, HP+N and HPHN conditions, respectively, for another 14 days prior to sampling. −P, 0.016 mM Pi; +P, 0.323 mM Pi; HP, 1.615 mM Pi; −N, 0.427 mM NO_3^-; +N, 1.425 mM NO_3^-; HN, 7.125 mM NO_3^-.

Measurement of Pi concentration in plants

Leaves and roots of the WT and transgenic seedlings from either Pi sufficient or Pi deficient treatments were sampled separately. The Pi concentration was measured using the procedure described previously (Delhaize and Randall, 1995). Briefly, 50 mg of fresh tissue samples was homogenized with 50 ml of 5 M H_2SO_4 and 3 ml of water. The homogenate was transferred to 1.5-ml tubes and centrifuged at 10 000 ***g*** for 10 min at 4°C. The supernatant was collected and diluted to an appropriate concentration. The diluted supernatant was mixed with a malachite green reagent in a 3:1 ratio and analyzed 20 min afterward. The absorption values for the solution at 650 nm were determined using a Spectroquant NOVA60 spectrophotometer (Merck, Darmstadt, Germany). Pi concentration was calculated from a standard curve generated with varying concentrations of KH_2PO_4.

RNA isolation and RT-PCR

Total RNA was extracted from plant samples using RNeasy Mini Kits according to the manufacturer's recommendations (Qiagen, Suzhou, China). First-strand cDNAs were synthesized from total RNA using SuperScript II reverse transcriptase (Invitrogen, CA, USA). The ACTIN cDNA is an endogenous control that is used to normalize the samples. The primers that were used for the RT-PCR are given in Table S1.

ACCESSION NUMBERS

Genes sequence in this article can be accessed from the MSU database with the following accession numbers: *O. sativa OsNLA1* (LOC_Os07g47590), *OsNLA2* (LOC_Os03g44810), *OsPHO2* (LOC_Os05g48390), *OsPT2* (LOC_Os03g05640) and *OsPT8* (LOC_Os10g30790).

ACKNOWLEDGEMENTS

This work was supported by the National Natural Science Foundation of China (31471929, 31401934 and 31572189), Ministry of Education (the '111 Project' of B14027), the Ministry of Science and Technology of China (2016YFD0100703), and the National Science Foundation of Zhejiang Province (LZ16C150001). The authors thank the Rice Genome Resource Center, Japan, for the Tos17 insertion mutants (NF5039 and NF0010).

CONFLICT OF INTEREST

The authors declare no conflict of interest.

SUPPORTING INFORMATION

Additional Supporting Information may be found in the online version of this article.

Figure S1. Protein sequence alignment of NLA, OsNLA1 and OsNLA2, and OsNLA1 protein structure.

Figure S2. Verification of homozygous *osnla1* mutants.

Figure S3. Growth performances of *osnla1* mutants, *OsNLA1*-overexpressing (OE) transgenic and the wild-type (NIP) plants under different conditions.

Figure S4. Transcript abundance of *OsPHR2* and *OsmiR827* in *OsPHR2*- and *OsmiR827*-overexpressing (OE) transgenic plants, *osnla1-2* and wild-type (NIP).

Figure S5. BiFC analysis for OsPHO2-cYFP or OsPHO2^{C719A}-cYFP with OsNLA1^{C265A}-nYFP in tobacco leaves.

Table S1. Primer sequences used in this study.

REFERENCES

Ai, P., Sun, S., Zhao, J. *et al.* (2009) Two rice phosphate transporters, OsPht1;2 and OsPht1;6, have different functions and kinetic properties in uptake and translocation. *Plant J.* **57**, 798–809.

Aung, K., Lin, S.I., Wu, C.C., Huang, Y.T., Su, C.L. and Chiou, T.J. (2006) pho2, a phosphate overaccumulator, is caused by a nonsense mutation in a microRNA399 target gene. *Plant Physiol.* **141**, 1000–1011.

Bari, R., Datt Pant, B., Stitt, M. and Scheible, W.R. (2006) PHO2, microRNA399, and PHR1 define a phosphate-signaling pathway in plants. *Plant Physiol.* **141**, 988–999.

Bieleski, R.L. (1973) Phosphate pools, phosphate transport, and phosphate availability. *Annu. Rev. Plant Physiol.* **24**, 225–252.

Bustos, R., Castrillo, G., Linhares, F., Puga, M.I., Rubio, V., Perez-Perez, J., Solano, R., Leyva, A. and Paz-Ares, J. (2010) A central regulatory system largely controls transcriptional activation and repression responses to phosphate starvation in Arabidopsis. *PLoS Genet.* **6**, e1001102.

Cao, Y., Yan, Y., Zhang, F., Wang, H.D., Gu, M., Wu, X.N., Sun, S.B. and Xu, G.H. (2014) Fine characterization of OsPHO2 knockout mutants reveals its key role in Pi utilization in rice. *J. Plant Physiol.* **171**, 340–348.

Chen, J., Liu, Y., Ni, J., Wang, Y., Bai, Y., Shi, J., Wu, Z. and Wu, P. (2011) OsPHF1 regulates the plasma membrane localization of low- and high-affinity Pi transporters and determines Pi uptake and translocation in rice. *Plant Physiol.* **111**, 181669.

Chen, J., Wang, Y., Wang, F. *et al.* (2015) The rice CK2 kinase regulates trafficking of phosphate transporters in response to phosphate levels. *Plant Cell*, **27**, 711–723.

Delhaize, E. and Randall, P.J. (1995) Characterization of a phosphate-accumulator mutant of Arabidopsis thaliana. *Plant Physiol.* **107**, 207–213.

Dou, H., Buetow, L., Sibbet, G.J., Cameron, K. and Huang, D.T. (2012) BIRC7-E2 ubiquitin conjugate structure reveals the mechanism of ubiquitin transfer by a RING dimer. *Nat. Struct. Mol. Biol.* **19**, 876–883.

Elmore, J.M. and Coaker, G. (2011) The role of the plasma membrane H+-ATPase in plant-microbe interactions. *Mol. Plant*, **4**, 416–427.

Gonzalez, E., Solano, R., Rubio, V., Leyva, A. and Paz-Ares, J. (2005) Phosphate transporter traffic facilitators1 is a plant-specific SEC12-related protein that enables the endoplasmic reticulum exit of a high-affinity phosphate transporter in Arabidopsis. *Plant Cell*, **17**, 3500–3512.

Guerra, D.D. and Callis, J. (2012) Ubiquitin on the move: the ubiquitin modification system plays diverse roles in the regulation of endoplasmic reticulum- and plasma membrane-localized proteins. *Plant Physiol.* **160**, 56–64.

Guo, B., Jin, Y., Wussler, C., Blancaflor, E.B., Motes, C.M. and Versaw, W.K. (2008) Functional analysis of the Arabidopsis PHT4 family of intracellular phosphate transporters. *New Phytol.* **177**, 889–898.

Hamburger, D., Rezzonico, E., MacDonald-Comber Petetot, J., Somerville, C. and Poirier, Y. (2002) Identification and characterization of the Arabidopsis PHO1 gene involved in phosphate loading to the xylem. *Plant Cell*, **14**, 889–902.

Huang, T.K., Han, C.L., Lin, S.I. *et al.* (2013) Identification of downstream components of ubiquitin-conjugating enzyme PHOSPHATE2 by quantitative membrane proteomics in Arabidopsis roots. *Plant Cell*, **25**, 4044–4060.

Hurlimann, H.C., Pinson, B., Stadler-Waibel, M., Zeeman, S.C. and Freimoser, F.M. (2009) The SPX domain of the yeast low-affinity phosphate transporter Pho90 regulates transport activity. *EMBO Rep.* **10**, 1003–1008.

Javot, H., Pumplin, N. and Harrison, M.J. (2007) Phosphate in the arbuscular mycorrhizal symbiosis: transport properties and regulatory roles. *Plant, Cell Environ.* **30**, 310–322.

Jia, H., Ren, H., Gu, M., Zhao, J., Sun, S., Zhang, X., Chen, J., Wu, P. and Xu, G. (2011) The phosphate transporter gene OsPht1;8 is involved in phosphate homeostasis in rice. *Plant Physiol.* **156**, 1164–1175.

Kant, S., Peng, M. and Rothstein, S.J. (2011) Genetic regulation by NLA and microRNA827 for maintaining nitrate-dependent phosphate homeostasis in arabidopsis. *PLoS Genet.* **7**, e1002021.

Karimi, M., Inz, D. and Depicker, A. (2002) GATEWAYTM vectors for Agrobacterium-mediated plant transformation. *Trends Plant Sci.* **7**, 193–195.

Lin, W.Y., Huang, T.K. and Chiou, T.J. (2013) Nitrogen limitation adaptation, a target of microRNA827, mediates degradation of plasma membrane-localized phosphate transporters to maintain phosphate homeostasis in Arabidopsis. *Plant Cell*, **25**, 4061–4074.

Liu, F., Chang, X.J., Ye, Y., Xie, W.B., Wu, P. and Lian, X.M. (2011) Comprehensive sequence and whole-life-cycle expression profile analysis of the phosphate transporter gene family in rice. *Mol. Plant*, **4**, 1105–1122.

Liu, T.Y., Huang, T.K., Tseng, C.Y., Lai, Y.S., Lin, S.I., Lin, W.Y., Chen, J.W. and Chiou, T.J. (2012) PHO2-dependent degradation of PHO1 modulates phosphate homeostasis in Arabidopsis. *Plant Cell*, **24**, 2168–2183.

Liu, T.Y., Huang, T.K., Yang, S.Y., Hong, Y.T., Huang, S.M., Wang, F.N., Chiang, S.F., Tsai, S.Y., Lu, W.C. and Chiou, T.J. (2016) Identification of plant vacuolar transporters mediating phosphate storage. *Nat. Commun.* **7**, 1–11.

Lv, Q., Zhong, Y., Wang, Y. *et al.* (2014) SPX4 negatively regulates phosphate signaling and homeostasis through its interaction with PHR2 in rice. *Plant Cell*, **26**, 1586–1597.

Nussaume, L., Kanno, S., Javot, H., Marin, E., Pochon, N., Ayadi, A., Nakanishi, T.M. and Thibaud, M.C. (2011) Phosphate import in plants: focus on the PHT1 transporters. *Front. Plant Sci.* **2**, 83.

Park, B.S., Seo, J.S. and Chua, N.H. (2014) NITROGEN LIMITATION ADAPTATION recruits PHOSPHATE2 to target the phosphate transporter PT2 for degradation during the regulation of Arabidopsis phosphate homeostasis. *Plant Cell*, **26**, 454–464.

Peng, M., Hannam, C., Gu, H., Bi, Y.M. and Rothstein, S.J. (2007) A mutation in NLA, which encodes a RING-type ubiquitin ligase, disrupts the adaptability of Arabidopsis to nitrogen limitation. *Plant J.* **50**, 320–337.

Peret, B., Desnos, T., Jost, R., Kanno, S., Berkowitz, O. and Nussaume, L. (2014) Root architecture responses: in search of phosphate. *Plant Physiol.* **166**, 1713–1723.

Prak, S., Hem, S., Boudet, J., Viennois, G., Sommerer, N., Rossignol, M., Maurel, C. and Santoni, V. (2008) Multiple phosphorylations in the C-terminal tail of plant plasma membrane aquaporins: role in subcellular trafficking of AtPIP2;1 in response to salt stress. *Mol. Cell Proteomics*, **7**, 1019–1030.

Secco, D., Wang, C., Shou, H. and Whelan, J. (2012) Phosphate homeostasis in the yeast Saccharomyces cerevisiae, the key role of the SPX domain-containing proteins. *FEBS Lett.* **586**, 289–295.

Shin, H., Shin, H.S., Dewbre, G.R. and Harrison, M.J. (2004) Phosphate transport in Arabidopsis: Pht1;1 and Pht1;4 play a major role in phosphate acquisition from both low- and high-phosphate environments. *Plant J.* **39**, 629–642.

Stefanovic, A., Arpat, A.B., Bligny, R., Gout, E., Vidoudez, C., Bensimon, M. and Poirier, Y. (2011) Over-expression of PHO1 in Arabidopsis leaves reveals its role in mediating phosphate efflux. *Plant J.* **66**, 689–699.

Tran, H.T., Hurley, B.A. and Plaxton, W.C. (2010) Feeding hungry plants: the role of purple acid phosphatases in phosphate nutrition. *Plant Sci.* **179**, 14–27.

Vance, C.P., Uhde-Stone, C. and Allan, D.L. (2003) Phosphorus acquisition and use: critical adaptations by plants for securing a nonrenewable resource. *New Phytol.* **157**, 423–447.

Walter, M., Chaban, C., Schutze, K. *et al.* (2004) Visualization of protein interactions in living plant cells using bimolecular fluorescence complementation. *Plant J.* **40**, 428–438.

Wang, C., Ying, S., Huang, H., Li, K., Wu, P. and Shou, H. (2009) Involvement of OsSPX1 in phosphate homeostasis in rice. *Plant J.* **57**, 895–904.

Wang, Z., Ruan, W., Shi, J. *et al.* (2014) Rice SPX1 and SPX2 inhibit phosphate starvation responses through interacting with PHR2 in a phosphate-dependent manner. *Proc. Natl Acad. Sci. USA*, **111**, 14953–14958.

Wang, C., Yue, W., Ying, Y., Wang, S., Secco, D., Liu, Y., Whelan, J., Tyerman, S.D. and Shou, H. (2015) Rice SPX-major facility duperfamily3, a vacuolar phosphate efflux transporter, is involved in maintaining phosphate homeostasis in rice. *Plant Physiol.* **169**, 2822–2831.

Wu, P., Shou, H., Xu, G. and Lian, X. (2013) Improvement of phosphorus efficiency in rice on the basis of understanding phosphate signaling and homeostasis. *Curr. Opin. Plant Biol.* **16**, 205–212.

Xie, Q., Guo, H.S., Dallman, G., Fang, S., Weissman, A.M. and Chua, N.H. (2002) SINAT5 promotes ubiquitin-related degradation of NAC1 to attenuate auxin signals. *Nature*, **419**, 167–170.

Yaeno, T. and Iba, K. (2008) BAH1/NLA, a RING-type ubiquitin E3 ligase, regulates the accumulation of salicylic acid and immune responses to Pseudomonas syringae DC3000. *Plant Physiol.* **148**, 1032–1041.

Yang, X., Baliji, S., Buchmann, R.C., Wang, H., Lindbo, J.A., Sunter, G. and Bisaro, D.M. (2007) Functional modulation of the geminivirus AL2 transcription factor and silencing suppressor by self-interaction. *J. Virol.* **81**, 11972–11981.

Zhou, J., Jiao, F., Wu, Z., Li, Y., Wang, X., He, X., Zhong, W. and Wu, P. (2008) OsPHR2 is involved in phosphate-starvation signaling and excessive phosphate accumulation in shoots of plants. *Plant Physiol.* **146**, 1673–1686.

